Pharm Res (2013) 30:1400–1408
DOI 10.1007/s11095-013-0978-7

RESEARCH PAPER

Preclinical Pharmacokinetic/Pharmacodynamic Models to Predict Schedule-Dependent Interaction Between Erlotinib and Gemcitabine

Mengyao Li • Hanqing Li • Xiaoliang Cheng • Xipei Wang • Liang Li • Tianyan Zhou • Wei Lu

Received: 9 July 2012 / Accepted: 7 January 2013 / Published online: 24 January 2013

ABSTRACT

Purpose To investigate the pharmacological effects of different erlotinib (ER) and gemcitabine (GM) combination schedules by *in vitro* and *in vivo* experiments and PK/PD models in non-small cell lung cancer cells.

Methods H1299 cells were exposed to different ER combined with GM schedules. Cell growth inhibition was analyzed to evaluate these schedules. A preclinical *in vivo* study was then conducted to compare tumor suppression effects of different schedules in H1299 xenografts. PK/PD models were developed to quantify the anti-tumor interaction of ER and GM.

Results Synergism was observed when ER preceded GM, but other sequences showed antagonism. The optimal *in vitro* schedule, or interval schedule, was applied to the animal study, which showed greater anti-tumor effect than simultaneous group. PK/PD models implied that interaction of the two drugs was additive in simultaneous treatment but synergistic in interval schedule. The simulation results showed that interval schedule can delay tumor growth for a longer time, and demonstrated more evident anti-tumor effect compared with simultaneous group if the treatment duration was longer.

Conclusions Interval schedule of the two drugs can achieve synergistic anti-tumor effect, and is superior to simultaneous treatment.

KEY WORDS combination · erlotinib · gemcitabine · interval schedule · PK/PD model

ABBREVIATIONS

EGFR	epidermal growth factor receptor
ER	erlotinib
FDA	Food and Drug Administration
FOCE	first order conditional estimation
GM	gemcitabine
MTD	maximum tolerated dose
NSCLC	non-small-cell lung cancer
OD	optical density
PBS	phosphate buffered saline
PK/PD	pharmacokinetic/pharmacodynamic
SRB	sulforhodamine B
TKI	tyrosine kinase inhibitor
VPC	visual predictive check

INTRODUCTION

Non-small-cell lung cancer (NSCLC) is the most common type of lung cancer, which accounts for 80–85% of lung cancer cases (1). Erlotinib (ER) is the first targeted therapeutic agent to treat advanced-stage NSCLC in clinic. It is an oral active, small-molecule tyrosine kinase inhibitor (TKI) that reversibly binds to the intracellular tyrosine kinase domain of epidermal growth factor receptor (EGFR). It can block the autophosphorylation of EGFR, and subsequently inhibit a series of down-signaling pathways, which then inhibit cell proliferation and angiogenesis. ER causes cells to accumulate in G1 phase and consequently induces tumor cells apoptosis (2,3). Gemcitabine (2′, 2′- difluorodeoxycytidine, GM) is a widely used chemotherapeutic agent for the treatment of NSCLC as well as pancreatic cancer (4). With a similar structure as cytosine arabinoside,

Electronic supplementary material The online version of this article (doi:10.1007/s11095-013-0978-7) contains supplementary material, which is available to authorized users.

L. Li • T. Zhou • W. Lu
State Key Laboratory of Natural and Biomimetic Drugs
Peking University, Beijing 100191, China

M. Li • H. Li • X. Cheng • X. Wang • L. Li • T. Zhou (✉) • W. Lu (✉)
Department of Pharmaceutics, School of Pharmaceutical Sciences
Peking University Health Science Center, Beijing 100191, China
e-mail: tianyanzhou@bjmu.edu.cn
e-mail: luwei_pk@bjmu.edu.cn

it can inhibit ribonucleotide reductase and be incorporated into the DNA, leading to chain termination ultimately (5). GM arrests cells mainly in S phase and induces apoptosis among a broad spectrum of solid tumors, including NSCLC.

ER and GM can both be used in the treatment of NSCLC, offering considerable potential to combine the two drugs and achieve better anti-tumor effects. A preclinical *in vivo* study (6) has shown that ER in combination with GM has an additive effect on tumor growth inhibition. However, some large, randomized phase III trials of continuous daily administration of ER in combination with chemotherapy doublets, including gemcitabine, have failed to improve survival in patients with advanced NSCLC (7-9). There is growing laboratory evidence supporting that EGFR TKIs induce G1-phase cell cycle accumulation, which protects cells from the S-phase arrest of chemotherapeutic agents (10,11). Therefore, separating the cell cycle arrests of EGFR TKIs and cytotoxicity agents can decrease the antagonism and maximize the combination effect.

Based on the hypothesis above, we aim to investigate the pharmacological effects of different ER and GM combination schedules *in vitro* and *in vivo*, and determine an optimal schedule with potential in clinical use. To better characterize and predict the pharmacological effects of various schedules, it is crucial to quantify the time course of pharmacodynamic responses in relation to plasma concentration (12), by developing pharmacokinetic/pharmacodynamic (PK/PD) mathematical models. Compared with traditional method to calculate combination index (13,14), PK/PD modeling is more suitable for the comparison across different treatment schemes and is applicable for characterizing combination effect of the whole time course besides that at the endpoint (12). The model-derived parameters can describe the potency of anticancer treatments, and assist in the selection of both optimal drug combinations and administration schedules, so as to maximize tumor suppression effect.

MATERIALS AND METHODS

Drugs and Reagents

ER was purchased from Shanghai Hanhong Chemical Co. Ltd (Shanghai, China) and GM was purchased from Beijing Lunarsun Pharmaceutical Co. Ltd (Beijing, China). Other chemicals were purchased from Sigma-Aldrich Co. (local agent, Beijing) unless otherwise indicated.

Cell Culture

Human NSCLC cell line H1299 was kindly provided by Dr. Zaiquan Li (School of Basic Medical Sciences, Peking University Health Science Center) and grown in RPMI1640 medium (Macgene Biotec Co., Ltd, Beijing, China) containing 10% fetal bovine serum (FBS, Macgene Biotech) and antibiotic (penicillin 100 UI/ml and streptomycin 100 μg/ml). Cells were maintained at 37°C in a humidified atmosphere of 95% air and 5% CO_2.

Cytotoxicity Assay

The sulforhodamine B (SRB) colorimetric assay was used to evaluate the growth inhibitory activity of drugs at various concentrations. Exponential growing H1299 cells were seeded in 96-well plastic plates at a density of 6×10^3 cells/well. Cells were incubated for 24 h to allow sufficient cell adhesion and one plate of cells was then taken out for fixation and staining without drug, which acted as the no-growth (day 0) group (15). Other plates were treated with serial dilutions of ER alone and GM alone for 48 h respectively in 6 replicated wells for each drug concentration. ER was dissolved and diluted with DMSO and GM was dissolved and diluted with phosphate buffered saline (137 mM NaCl, 2.7 mM KCl, 8 mM Na_2HPO_4, and 2 mM KH_2PO_4, PBS, pH 7.4). The control group of ER was exposed to the same volume of DMSO, and the control group of GM was added the same volume of PBS. After incubation for 48 h, cells were fixed with 10% (wt/vol) trichloroacetic acid and stained with 0.4% (wt/vol) SRB (dissolved in 1% acetic acid) for 30 min. The protein-bound dye was subsequently dissolved in 10 mmol/L Tris (pH = 10.5) and the absorbance at 540 nm was read on colorimetric plate reader (15).

Growth inhibition was expressed as the following equation (Eq. 1):

$$\%\ of\ control\ cell\ growth = \frac{mean\ OD_{sample} - mean\ OD_{day\,0}}{mean\ OD_{control} - mean\ OD_{day\,0}} \times 100 \quad (1)$$

All results obtained from the SRB assay fell within the linearity limit (up to OD 1.5–2.0 (15)). The IC_{50} value was the concentration resulting in 50% cell growth inhibition by a 48 h exposure to drug compared with untreated control cells.

Analysis of Drug Combination Effects

To investigate combination effects of ER and GM, cells were treated with six different schedules: (A) simultaneous exposure of ER and GM for 24 h followed by drug-free medium for 24 h; (B) simultaneous exposure of ER and GM for 48 h; (C) sequential exposure of ER for 24 h followed by simultaneous exposure of ER and GM for 24 h; (D) sequential exposure of ER for 24 h, aspirated and washed once with drug-free medium, followed by GM for 24 h; (E) sequential exposure of GM for 24 h followed by simultaneous exposure of GM and

ER for 24 h; (F) sequential exposure of GM for 24 h, aspirated and washed once with drug-free medium, followed by ER for 24 h (Fig. 1). ER and GM were combined at a fixed concentration ratio of 100:1, determined based on the IC_{50} value of each drug in H1299 (16,17). The interaction between the drugs was evaluated using the published methods (18,19), based on the principles described by Chou *et al.* (14). In brief, the expected value of combination effect between ER and GM was calculated as followed (Eq. 2):

$$Expected\ value = \frac{ER\ value}{control\ value} \times \frac{GM\ value}{control\ value} \times control\ value \quad (2)$$

ER value and GM value were the cell survival rates of ER, GM single group; control value was 100% here. The combination index (CI) was calculated as the ratio of (expected value)/(observed value). CI < 1 indicates a synergistic effect; CI = 1 indicates an additive effect; CI > 1 indicates an antagonistic effect.

In Vivo Pharmacodynamic Studies

Female BALB/c nude mice (16–18 g) were purchased from the Experimental Animal Center, Peking University Health Science Center. All animal studies were approved by the Institutional Animal Care and Use Committee. 9×10^6 H1299 cells were suspended in 200 μL PBS, and inoculated subcutaneously in mice's right flank. Tumor diameter was measured with vernier caliper and converted to tumor volume using the formula length × width^2/2 (20). When tumor size reached 150–250 mm^3, mice were randomly assigned to different treatment groups: (a) vehicle control group. (b) ER (12.5 mg/kg) group: ER was dissolved in 4% SBE-β-CD Captisol solution and administered by gavage. (c) GM (20 mg/kg) group: GM was dissolved in PBS (pH = 7.4) and administered via intravenous injection. (d) Simultaneous group: ER (12.5 mg) was administered concurrently with GM (20 mg/kg). (e) Interval group: GM (20 mg/kg) was administered 18 h after ER (12.5 mg/kg) was given. Four percent SBE-β-CD or ER was administered daily, PBS or GM was administered every 3 days. Treatments lasted for 2 weeks and tumor growth inhibition rate was calculated with the formula (Eq. 3):

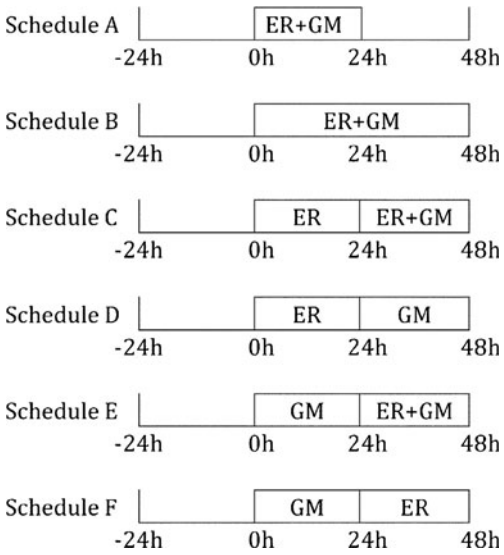

Fig. 1 Schematic of the six combination schedules tested in cytotoxicity assay.

$$R_V = 100\% - \frac{V_{drug}}{V_{vehicle}} \times 100\% \quad (3)$$

where V_{drug} was the tumor volume after treated with drug, and $V_{vehicle}$ was the tumor volume after treated with vehicle.

Pharmacokinetic Study

A LC-MS/MS method was developed by our group previously, to determine the pharmacokinetics of ER in female BALB/c nude mice plasma (21). According to the study, ER was dosed by gavage at 12.5 mg/kg and plasma samples were collected at various time points. The PK parameters of ER were extracted from our previous study (21). The PK parameters of GM were taken from literature (22).

PK/PD Linked Models

The tumor growth curves were analyzed using the model introduced by Simeoni *et al.* (23) and modified by Koch *et al.* (12). The tumor growth in non-treated animals was described by an exponential phase followed by a linear growth phase. A nonlinear tumor growth function (Eq. 4) is applied to fit the consistent observed tumor growth data, in which λ_0 represents the exponential growth rate, λ_1 denotes the linear growth rate. All the cells are assumed to be proliferating in the vehicle control group.

$$f(X_1) = \frac{2\lambda_0\lambda_1 X_1}{\lambda_1 + 2\lambda_0 X_1} \quad (4)$$

In the single drug groups, it is assumed that the anticancer treatment makes some cells non-proliferating and eventually brings them to death through a mortality chain (Fig. 2a). The portion of proliferating cells within the total tumor volume is denoted as X_1. The plasma concentration of anticancer agent is represented as C(t). The rate from proliferating to non-proliferating cells (X_2, X_3, X_4) is in proportion with drug concentration in plasma (12,24,25), with a factor of k_2, which describes the anti-tumor potency of the compound. To characterize the time delay between drug exposure and drug effect, a transit compartment model

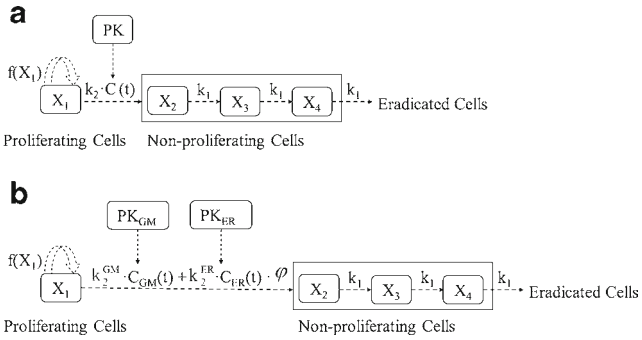

Fig. 2 (**a**) PK/PD model structure of single drug. (**b**) PK/PD model structure of different combination schedules.

(23,25-27) has been used and k_1 is the transit-rate constant between several non-proliferating compartments. v(t) is the sum of volume of the cells in various stages. The differential equations are as follows (Eqs. 5–9):

$$\frac{dX_1}{dt} = \frac{2\lambda_0\lambda_1 X_1(t)^2}{(\lambda_1 + 2\lambda_0 X_1(t))v(t)} - k_2 C(t) X_1(t),\ X_1(0) = v_0 \quad (5)$$

$$\frac{dX_2}{dt} = k_2 C(t) X_1(t) - k_1 X_2(t),\ X_2(0) = 0 \quad (6)$$

$$\frac{dX_3}{dt} = k_1 (X_2(t) - X_3(t)),\ X_3(0) = 0 \quad (7)$$

$$\frac{dX_4}{dt} = k_1 (X_3(t) - X_4(t)),\ X_4(t) = 0 \quad (8)$$

$$v_t = X_1 + X_2 + X_3 + X_4 \quad (9)$$

where λ_0 and λ_1 are the same with vehicle control group, and v_0 (the initial tumor volume) is estimated for each group.

In the combination groups, we extended the PK/PD model using parameters k_2^{ER} and k_2^{GM} representing the potency of ER and GM, which are estimated from monotherapy. Then, a combination index φ is introduced to determine the interaction of joint administration, and the total influence on tumor growth denotes as $\left(k_2^{GM} \cdot C_{GM}(t) + k_2^{ER} \cdot C_{ER}(t) \cdot \varphi\right)$. The φ value greater or less than 1 signifies the degree of increase or decrease in antitumor effect. Therefore, the combination index can indicate synergism or antagonism of the two drugs. The model structure is shown in Fig. 2b with the following equations (Eqs. 10–14):

$$\frac{dX_1}{dt} = \frac{2\lambda_0\lambda_1 X_1(t)^2}{(\lambda_1 + 2\lambda_0 X_1(t))v(t)} - \left(k_2^{GM} C_{GM}(t) + k_2^{ER} C_{ER}(t) \cdot \varphi\right) X_1(t),$$
$$X_1(0) = v_0 \quad (10)$$

$$\frac{dX_2}{dt} = \left(k_2^{GM} C_{GM}(t) + k_2^{ER} C_{ER}(t) \cdot \varphi\right) X_1(t) - k_1 X_2(t),$$
$$X_2(0) = 0 \quad (11)$$

$$\frac{dX_3}{dt} = k_1 (X_2(t) - X_3(t)),\quad X_3(0) = 0 \quad (12)$$

$$\frac{dX_4}{dt} = k_1 (X_3(t) - X_4(t)),\quad X_4(t) = 0 \quad (13)$$

$$v_t = X_1 + X_2 + X_3 + X_4 \quad (14)$$

where k_2^{GM} and k_2^{ER} fix to *a priori*, but k_1 differs from monotherapy groups.

Data Analysis and Model Simulations

The PK parameters of ER (21) and GM (22) were used to simulate the plasma concentration time profiles according to different treatment schedules. The vehicle control group predicts the rates of tumor growth (λ_0 and λ_1), which are fixed in treated groups. The model estimations were performed using NONMEM 7 (level 1.0) with FOCE method. Both interindividual and residual variability were added into the models. We assumed that the parameters and residual errors variability followed logarithmic normal distribution, and the residual error model was multiplicative error model. Model validations were based on visual predictive check (VPC) of the predictions with 1,000 times simulations by using PsN (version 3.4.2). Relative standard errors (RSE) were provided to evaluate the precision of parameters. With these model parameters, the tumor size-time profiles of different schedules dosed from day 0 to day 16 according to the *in vivo* experiments were simulated, as well as the tumor growth curves of two combination schedules treated for 70 days. v_0 of different schedules was fixed at the same value for between-group comparison.

Statistical Analysis

The results were presented as mean±SD. One-way analysis of variance (ANOVA) was used to determine the significance among groups, after which post hoc tests with the Bon-Ferroni's correction were used for multiple comparisons

between individual groups. Difference at a level of $P<0.05$ was considered statistically significant.

RESULTS

Cytotoxicity of ER, GM Alone, or in Combination

The cytotoxicity effects of ER and GM on H1299 were found to be dose-dependent according to our study. The IC_{50} value was 19.18 μM for ER and 0.22 μM for GM. Concentration of ER > 20 μmol/L could not be achieved because of the low solubility of ER in culture medium. Therefore, ER's maximum concentration was set to 20 μM in combination schedules. The cytotoxicity and CI values of six schedules were shown in Fig. 3a and b. The inhibition effects of simultaneous administrations (Schedule A and Schedule B) were similar to or even poorer than those of single-drug experiments, and CI values in schedule A ranged from 1 to 4.5, indicating a marked antagonism. In contrast, when cells were treated with ER followed by GM (Schedule C and Schedule D), especially in Schedule D, the growth of H1299 cells was significantly inhibited. Besides, removing ER before the addition of GM, or namely interval schedule, demonstrated greater cytotoxicity effect. The CI values ranged from 1.1 to −2.98 and decreased with the concentration getting higher. The maximum concentration of ER and GM not only inhibited the growth of cells, but also killed original tumor cells. The GM→ER sequence treatments (Schedule E and Schedule F) demonstrated no better cytotoxicity effect as compared to concurrent schedules, which resulted in antagonism in the effective concentration range.

Inhibitory Effect of Different Schedules on H1299 Xenografts

The optimal *in vitro* schedule—interval schedule (Schedule D)—was applied to the treatment of H1299 xenografts in BALB/c nude mice, and the anti-tumor effect was compared with traditional monotherapy and simultaneous drug schedule. Figure 4a and b showed the tumor inhibition effects of various schedules on H1299 xenografts and the picture of excised tumors on day 30. Compared with

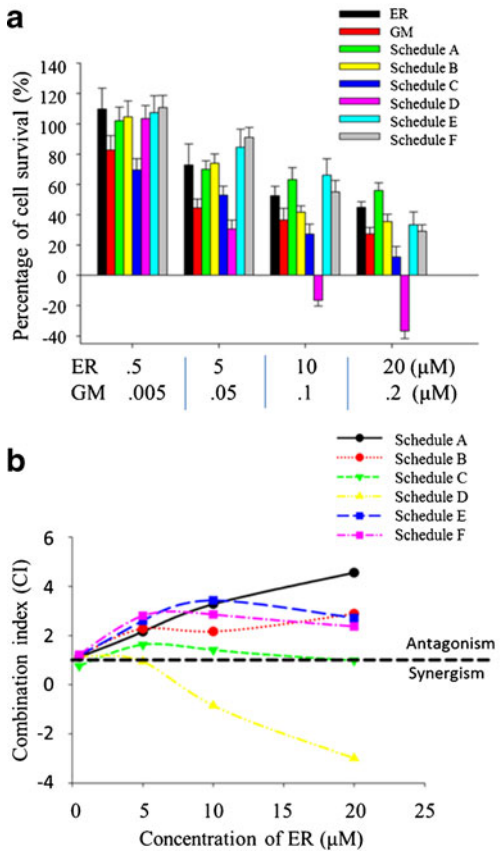

Fig. 3 Cytotoxic interaction of ER and GM. (**a**) Cells were incubated with increasing concentrations of ER and GM alone or combined at a concentration ratio of 100:1. Values were expressed as means ± SD of six experiments ($n = 6$). (**b**) The combination index defining the interaction between ER and GM was plotted against the concentrations of ER.

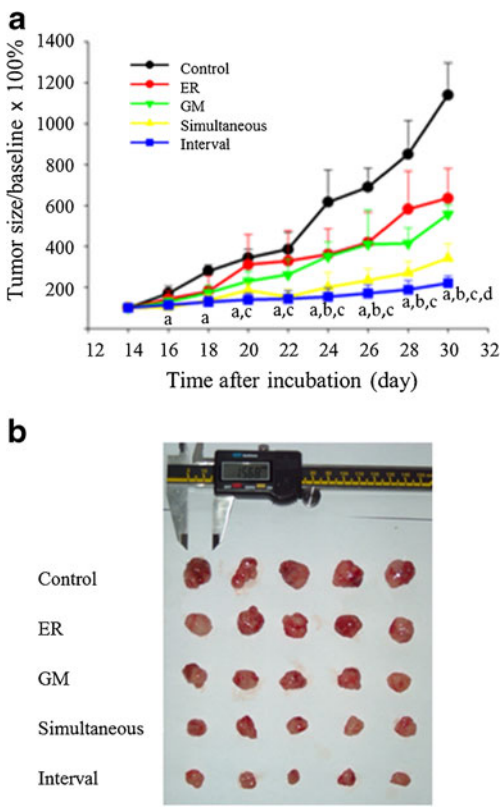

Fig. 4 (**a**) Antitumor efficacy of different schedules in H1299 xenografts in female BALB/c nude mice. Data were presented as the mean ± SD ($n = 5$). (**b**) Picture of excised tumors on day 30. a, $P < 0.05$, *versus* vehicle control; b, $P < 0.05$, *versus* ER; c, $P < 0.05$, *versus* GM; d, $P < 0.05$, *versus* simultaneous schedule.

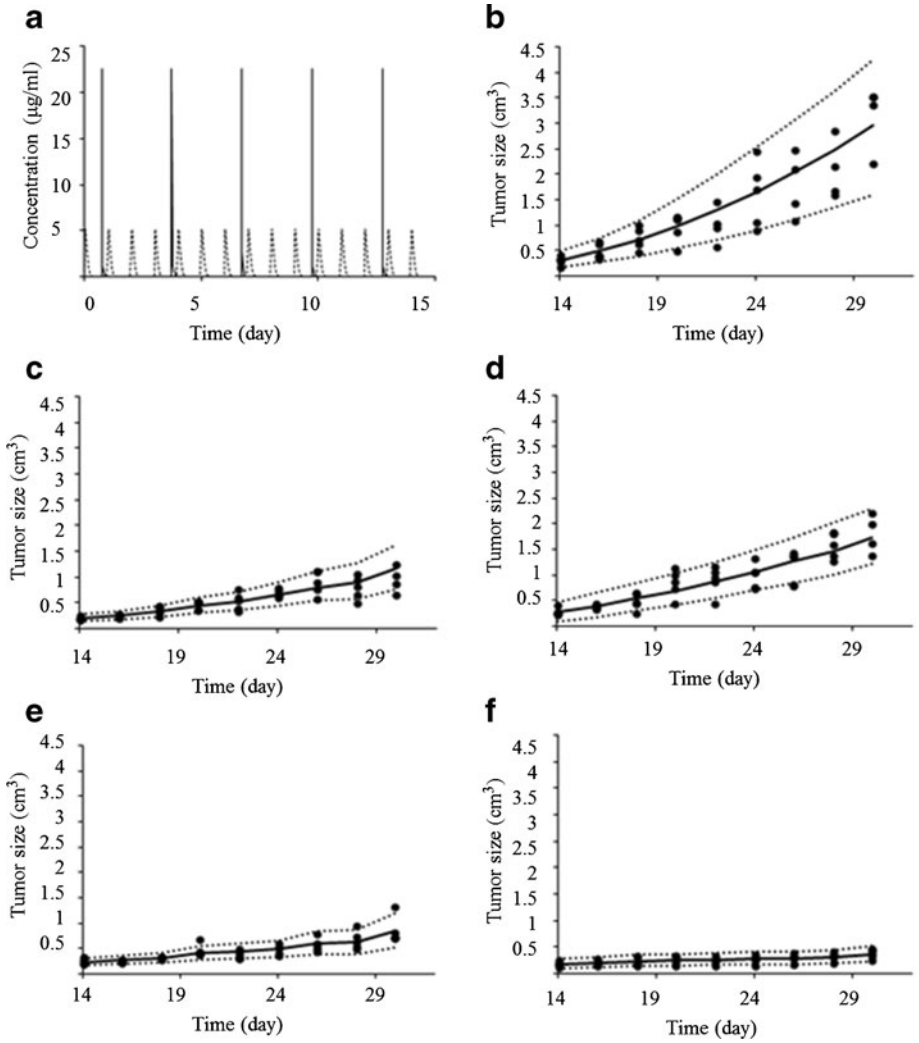

Fig. 5 (**a**) Simulated concentration—time profile of interval group. The *solid line* was the simulation of GM PK. The *dashed line* was the simulation of ER PK. (**b**–**f**) Observed and predicted tumor size—time profiles of different groups. The range between the dotted lines depicted the 90% confidence intervals. The *solid line* represented the medians of simulated data. The *solid dots* were the observed data. (**b**) Vehicle control group. (**c**) GM group. (**d**) ER group. (**e**) Simultaneous group. (**f**) Interval group.

monotherapy, simultaneous group showed increased inhibition of tumor growth, but the tumor inhibition of interval group was better than simultaneous group after drug administration for 16 days. The tumor volume inhibition rate at day 30 was 44.22±12.74% for ER alone, 51.10±4.08 for GM alone, 69.96±6.32% for simultaneous group and 80.66±3.17 for interval group. The tumor size—time profiles of different schedules were applied to PK/PD model as pharmacodynamic data.

Table I PK Parameters Extracted from Literatures

Parameters	GM	ER
CL ($ml \cdot kg^{-1} \cdot day^{-1}$)	84500	19032
V_c ($ml \cdot kg^{-1}$)	887	885
Q ($ml \cdot kg^{-1} \cdot day^{-1}$)	53100	763.2
V_p ($ml \cdot kg^{-1}$)	970	168
k_a (day^{-1})	–	22.6

PK/PD Models of Different Schedules

The pharmacokinetics of ER was described by an extravascular two-compartment model with first order absorption kinetics (21) and GM was fitted well with a two-compartment model (22). With PK parameters, we simulated the PK data according to different pharmacodynamic schedules, and developed a PD model for vehicle control group and PK/PD models for treated groups. The simulated concentration—time profile of interval group was shown in Fig. 5a. The results of fitting tumor size—time data were shown in Fig. 5b–f. All the models fit well with the observed pharmacodynamic profiles, and most observed values were within the range of 90% confidence interval of predictions. The PK parameters and PD estimates were displayed in Tables I and II respectively. The exponential growth rate λ_0 was 0.137 day^{-1} and the linear growth rate λ_1 was 0.335 $cm^3 \cdot day^{-1}$. We hypothesized that each drug only influenced the rate from proliferating compartment to non-proliferating compartment, and didn't influence the cell

Table II PD Estimates Obtained from PK/PD Models

Parameters	Control (RSE%)	ER (RSE%)	GM (RSE%)	Simultaneous (RSE%)	Interval (RSE%)
v_0 (cm^3)	0.319 (13.3)	0.270 (16.6)	0.204 (6.97)	0.242 (6.98)	0.168 (14.5)
λ_0 (day^{-1})	0.137 (27.6)	0.137[a]	0.137[a]	0.137[a]	0.137[a]
λ_1 ($cm^3 \cdot day^{-1}$)	0.335 (10.4)	0.335[a]	0.335[a]	0.335[a]	0.335[a]
k_2^{GM} ($ml \cdot \mu g^{-1} \cdot day^{-1}$)	–	–	0.924 (8.13)	0.924[a]	0.924[a]
k_2^{ER} ($ml \cdot \mu g^{-1} \cdot day^{-1}$)	–	0.0716 (16.5)	–	0.0716[a]	0.0716[a]
k_1 (day^{-1})	–	0.544 (20.6)	1.96 (14.3)	3.66 (36.6)	1.75 (21.0)
φ	–	–	–	0.961 (15.9)	1.82 (12.4)

[a] Fixed in modeling process

growth rate in proliferating cells. Thus, we fixed λ_0 and λ_1 in the drug treatment groups with the same values of control group. k_2 was 0.924 $ml \cdot \mu g^{-1} \cdot day^{-1}$ for GM and 0.0716 $ml \cdot \mu g^{-1} \cdot day^{-1}$ for ER, suggesting that GM had stronger anti-tumor potency than ER. k_1 was 1.96 day^{-1} for GM and 0.544 day^{-1} for ER, indicating that ER took effect slower than GM and the anti-tumor effect of ER delayed for a longer time than GM. φ of simultaneous treatment and interval schedule were 0.961 and 1.82 respectively, which implied that interaction of the two drugs was additive in simultaneous treatment and synergistic in interval schedule. RSEs of parameters were lower than 30% except k_1 of simultaneous group, indicating high precision of model estimations.

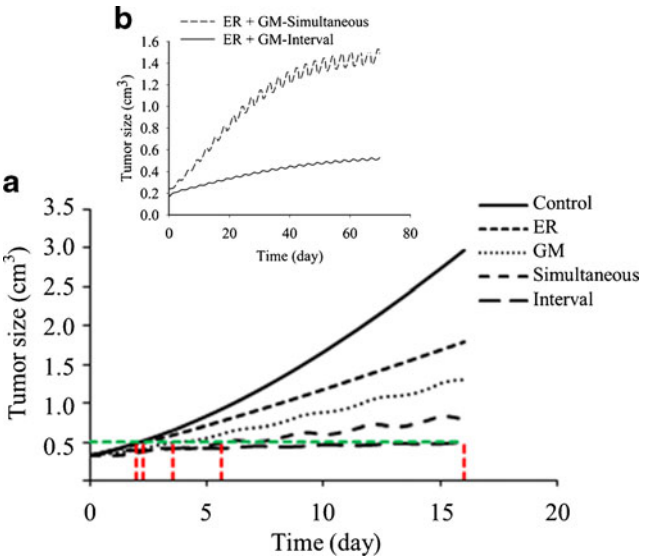

Fig. 6 (**a**) Simulated tumor size—time profile of BALB/c nude mice after multiple doses of different drug schedules from day 0 to day 16. The *black lines* depicted the tumor growth curves with different drug schedules, the *green dash line* represented the tumor size of 0.48 cm^3, the *red dashed lines* represented the time points to reach tumor-size of 0.48 cm^3 after different schedules. (**b**) Simulated tumor size—time profiles of BALB/c nude mice after ER+GM simultaneous schedule or ER+GM interval schedule for 70 days.

Model Simulations

Figure 6a showed the simulated tumor size—time profiles of different schedules dosed from day 0 to day 16 according to the *in vivo* experiments. The green dash line represented the tumor size of 0.48 cm^3, the red dashed lines represented the time points to reach tumor-size of 0.48 cm^3 under different treatments. The time point of reaching 0.48 cm^3 was 2d for control group, 2.3d for ER group, 3.5d for GM group, 5.6d for simultaneous group and 16d for interval group, which meant that interval group can delay tumor growth for 14d. When comparing the two combination treatments for a longer duration (Fig. 6b), the interval group demonstrated more evident anti-tumor effect than the simultaneous group, with a steady-state tumor volume of 0.54 cm^3 after dosing for 65d. The fluctuation of tumor volume was also less for interval schedule.

DISCUSSION

This is the first systemic preclinical study of combination of ER and GM in NSCLC cell lines. Initially, we started with testing if the *in vitro* antiproliferative activity of ER and GM in combination was sequence-dependent. In H1299 cells, Schedule D-delivering ER and GM sequentially—advantaged other schedules, and showed synergistic effect. However, in GM→ER treatment, Schedule F-two drugs also delivered separately—didn't show superiority in cytotoxicity effect, which may be a result of different sensitivity of H1299 to ER and GM (10,17). Therefore, in the *in vitro* studies, sequential delivery of ER followed by GM was the optimal schedule, thus necessary to be tested *in vivo*.

An *in vivo* tumor suppression experiment was then conducted on H1299 xenografts in BALB/c female nude mice. To administer the two drugs separately *in vivo*, we designed the interval schedule according to half-life time of each drug. $T_{1/2}$ of ER is 4.5 h with 1 h absorption time in BALB/c nude mice (21); $t_{1/2}$ of GM is 12 min in BALB/c nude mice (22). Therefore if GM was dosed 18 h after ER, the interval time

can allow ER and GM to eliminate to below 1/10 of their peak concentrations before the next dose of GM or ER, which was consistent with our simulation result (Fig. 5a). Tumor inhibition of interval group was significantly better than simultaneous group after drugs administration for 16 days, which confirmed that the interval schedule reduced antagonism between the two drugs in H1299 cells. Different from the *in vitro* antiproliferative results, simultaneous group showed additive anti-tumor interaction in the two drugs. A confounding factor here is that our doses of ER and GM were far less than their MTD in nude mice, which were 100 mg/kg for ER and 120 mg/kg for GM (6). Antagonistic effect of erlotinib and chemotherapeutic agents was reported only at their MTD (6). Therefore, it is possible that at doses lower than MTD, the antagonistic interaction between the two drugs was not shown.

Further, we developed PK/PD models to describe and predict tumor suppression effect of different schedules. The *in vivo* tumor growth profiles were applied to models as the pharmacodynamic data. Due to the limitation of nude mice, it is difficult to obtain the pharmacokinetic and pharmacodynamic data from the same animal; therefore, we decided to estimate PD parameters with PK parameters fixed at literature values. Both ER and GM have relatively short elimination half-time (21,22), thus showed no accumulation with the dose interval in our schemes. It makes sense to obtain the PK parameters from single-dose experiments, and simulate the PK profiles according to corresponding pharmacodynamic trial courses. Meanwhile, the possibility of significant pharmacokinetic interaction between the two drugs should also be excluded. Although no published paper has investigated the pharmacokinetic interaction between ER and GM in nude mice, FDA drug label claims that no significant interaction is observed between erlotinib and gemictibine in human (28). In addition, ER is mainly metabolized by CYP3A4 both in human and nude mice (29); GM is metabolized intracellularly by nucleoside kinases, and eliminated through renal excretion (30), which is also the same in the two species. Therefore, we can assume that there is no significant pharmacokinetic interaction between the two drugs. The PK parameters of ER were obtained from a previous study conducted by our group (21). GM PK parameters were extracted from literature (22), with the same animal strains, dosage form, and route of administration as our study. Therefore the extracted data can well describe pharmacokinetic profile of GM in our research.

In monotherapy PK/PD models, tumor suppression effect was determined by both k_2 (natural potency) and k_1 (transit rate). As k_2 of GM was larger, GM demonstrated stronger anti-tumor potency, which was consistent with the *in vitro* cytotoxicity result that H1299 is more sensitive to GM than ER. Meanwhile, as k_1 of ER was smaller, it took a relatively longer time for ER to take tumor suppression effect, which can be explained by its antitumor mechanism. ER is a therapeutic agent targeted to EGFR, and sequentially inhibits a series of down-signaling pathways. Therefore ER has delayed anti-tumor effect and can stop cell proliferation over a period of time rather than only showing instant effect. In combination therapy PK/PD models, we placed φ only on one drug according to literature (12). Actually, wherever φ was added, it indicated synergism between the two drugs if it was larger than 1. There is no confirmed mechanism of the phamacodynamic interaction between the two drugs, so we decided to place φ on ER, as this model had a lower objective function value during estimation. According to φ of two combination treatments, interval schedule led to synergistic effect of instant cell antiproliferation, while simultaneous schedule led to additive interaction. The anti-tumor effect of interval schedule showed evident hysteresis and can last for longer time. One limitation here was that k_1 of the combination therapies cannot be predicted from single agent exposures, thus it had to be estimated separately in each treatment. The simulation results also implied that interval schedule can delay tumor growth for the longest time and its advantage in antitumor effect compared to traditional simultaneous treatments increased as the dose duration prolongs. In addition, possible toxicity of long duration administration should be taken into consideration. From this analysis, we can infer that the model parameters are related to tumor growth characteristics, drug potency, and the kinetics of the tumor cell death, thus they can provide insights for drug mechanisms and behaviors. Simulations based on model estimates can also potentially guide clinical medication. It is recommended that erlotinib and gemcitabine may be sequentially combined with interval in clinic, but there is still a need to further exam the interval time.

CONCLUSION

Both the experimental and modeling results suggested that ER and GM achieve synergism in anti-tumor effect in the interval schedule of ER followed by GM, which was superior to traditional simultaneous treatment. The interval schedule has some indications for clinical medication. The PK/PD models in this study can be applied to standard xenograft experiments and may assist in the selection of both optimal drug combinations and administration schedules.

ACKNOWLEDGMENTS AND DISCLOSURES

This work was supported by the Ministry of Science and Technology of the People's Republic of China Grant 2009ZX09301-010 and National Natural Science Foundation of China (NSFC) Grant 81273583.

REFERENCES

1. Jemal A, Thun MJ, Ries LA, Howe HL, Weir HK, Center MM, Ward E, Wu XC, Eheman C, Anderson R, Ajani UA, Kohler B, Edwards BK. Annual report to the nation on the status of cancer, 1975–2005, featuring trends in lung cancer, tobacco use, and tobacco control. J Natl Cancer Inst. 2008;100(23):1672–94.
2. Mendelsohn Jand Baselga J. Status of epidermal growth factor receptor antagonists in the biology and treatment of cancer. J Clin Oncol. 2003;21(14):2787–99.
3. Perez-Soler R. HER1/EGFR targeting: refining the strategy. Oncologist. 2004;9(1):58–67.
4. Meyer F, Lueck A, Hribaschek A, Lippert H, Ridwelski K. Phase I trial using weekly administration of gemcitabine and docetaxel in patients with advanced pancreatic carcinoma. Chemotherapy. 2004;50(6):289–96.
5. Huang P, Chubb S, Hertel LW, Grindey GB, Plunkett W. Action of 2′,2′-difluorodeoxycytidine on DNA synthesis. Cancer Res. 1991;51(22):6110–7.
6. Higgins B, Kolinsky K, Smith M, Beck G, Rashed M, Adames V, Linn M, Wheeldon E, Gand L, Birnboeck H, Hoffmann G. Antitumor activity of erlotinib (OSI-774, Tarceva) alone or in combination in human non-small cell lung cancer tumor xenograft models. Anticancer Drugs. 2004;15(5):503–12.
7. Gatzemeier U, Pluzanska A, Szczesna A, Kaukel E, Roubec J, De Rosa F, Milanowski J, Karnicka-Mlodkowski H, Pesek M, Serwatowski P, Ramlau R, Janaskova T, Vansteenkiste J, Strausz J, Manikhas GM, Von Pawel J. Phase III study of erlotinib in combination with cisplatin and gemcitabine in advanced non-small-cell lung cancer: the Tarceva Lung Cancer Investigation Trial. J Clin Oncol. 2007;25(12):1545–52.
8. Herbst RS, Prager D, Hermann R, Fehrenbacher L, Johnson BE, Sandler A, Kris MG, Tran HT, Klein P, Li X, Ramies D, Johnson DH, Miller VA. TRIBUTE: a phase III trial of erlotinib hydrochloride (OSI-774) combined with carboplatin and paclitaxel chemotherapy in advanced non-small-cell lung cancer. J Clin Oncol. 2005;23(25):5892–9.
9. Stinchcombe TE, Peterman AH, Lee CB, Moore DT, Beaumont JL, Bradford DS, Bakri K, Taylor M, Crane JM, Schwartz G, Hensing TA, McElroy Jr E, Niell HB, Harper HD, Pal S, Socinski MA. A randomized phase II trial of first-line treatment with gemcitabine, erlotinib, or gemcitabine and erlotinib in elderly patients (age >/=70 years) with stage IIIB/IV non-small cell lung cancer. J Thorac Oncol. 2011;6(9):1569–77.
10. Giovannetti E, Lemos C, Tekle C, Smid K, Nannizzi S, Rodriguez JA, Ricciardi S, Danesi R, Giaccone G, Peters GJ. Molecular mechanisms underlying the synergistic interaction of erlotinib, an epidermal growth factor receptor tyrosine kinase inhibitor, with the multitargeted antifolate pemetrexed in non-small-cell lung cancer cells. Mol Pharmacol. 2008;73(4):1290–300.
11. Morelli MP, Cascone T, Troiani T, De Vita F, Orditura M, Laus G, Eckhardt SG, Pepe S, Tortora G, Ciardiello F. Sequence-dependent antiproliferative effects of cytotoxic drugs and epidermal growth factor receptor inhibitors. Ann Oncol. 2005;16 Suppl 4:iv61–8.
12. Koch G, Walz A, Lahu G, Schropp J. Modeling of tumor growth and anticancer effects of combination therapy. J Pharmacokinet Pharmacodyn. 2009;36(2):179–97.
13. Drewinko B, Loo TL, Brown B, Gottlieb JA, Freireich EJ. Combination chemotherapy *in vitro* with adriamycin. Observations of additive, antagonistic, and synergistic effects when used in two-drug combinations on cultured human lymphoma cells. Cancer Biochem Biophys. 1976;1(4):187–95.
14. Chou TC, Talalay P. Quantitative analysis of dose-effect relationships: the combined effects of multiple drugs or enzyme inhibitors. Adv Enzyme Regul. 1984;22:27–55.
15. Vichai Vand Kirtikara K. Sulforhodamine B colorimetric assay for cytotoxicity screening. Nat Protoc. 2006;1:1112–6.
16. Cheng H, An SJ, Zhang XC, Dong S, Zhang YF, Chen ZH, Chen HJ, Guo AL, Lin QX, Wu YL. *In vitro* sequence-dependent synergism between paclitaxel and gefitinib in human lung cancer cell lines. Cancer Chemother Pharmacol. 2011;67(3):637–46.
17. Li T, Ling YH, Goldman ID, Perez-Soler R. Schedule-dependent cytotoxic synergism of pemetrexed and erlotinib in human non-small cell lung cancer cells. Clin Cancer Res. 2007;13(11):3413–22.
18. Ceresa C, Giovannetti E, Voortman J, Laan AC, Honeywell R, Giaccone G, Peters GJ. Bortezomib induces schedule-dependent modulation of gemcitabine pharmacokinetics and pharmacodynamics in non-small cell lung cancer and blood mononuclear cells. Mol Cancer Ther. 2009;8(5):1026–36.
19. Mai Z, Blackburn GL, Zhou JR. Soy phytochemicals synergistically enhance the preventive effect of tamoxifen on the growth of estrogen-dependent human breast carcinoma in mice. Carcinogenesis. 2007;28(6):1217–23.
20. Son DS, Wilson AJ, Parl AK, Khabele D. The effects of the histone deacetylase inhibitor romidepsin (FK228) are enhanced by aspirin (ASA) in COX-1 positive ovarian cancer cells through augmentation of p21. Cancer Biol Ther. 2010;9(11):928–35.
21. Li M, Wu Q, Li HQ, Ning MR, Chen Y, Li L, Zhou TY, Lu W. A sensitive LC-MS/MS method to determine the concentrations of erlotinib and its active metabolite OSI-420 in BALB/c nude mice plasma simulatneously and its application to a pharmacokinetic study. J Chin Pharmaceut Sci. 2012;21:296–303.
22. Immordino ML, Brusa P, Rocco F, Arpicco S, Ceruti M, Cattel L. Preparation, characterization, cytotoxicity and pharmacokinetics of liposomes containing lipophilic gemcitabine prodrugs. J Control Release. 2004;100(3):331–46.
23. Simeoni M, Magni P, Cammia C, De Nicolao G, Croci V, Pesenti E, Germani M, Poggesi I, Rocchetti M. Predictive pharmacokinetic-pharmacodynamic modeling of tumor growth kinetics in xenograft models after administration of anticancer agents. Cancer Res. 2004;64(3):1094–101.
24. Jusko WJ. Pharmacodynamics of chemotherapeutic effects: dose-time-response relationships for phase-nonspecific agents. J Pharm Sci. 1971;60(6):892–5.
25. Bernard A, Kimko H, Mital D, Poggesi I. Mathematical modeling of tumor growth and tumor growth inhibition in oncology drug development. Expert Opin Drug Metab Toxicol; 2012.
26. Rocchetti M, Simeoni M, Pesenti E, De Nicolao G, Poggesi I. Predicting the active doses in humans from animal studies: a novel approach in oncology. Eur J Cancer. 2007;43(12):1862–8.
27. Yang J, Mager DE, Straubinger RM. Comparison of two pharmacodynamic transduction models for the analysis of tumor therapeutic responses in model systems. AAPS J. 2010;12(1):1–10.
28. Cohen MH, Johnson JR, Chen YF, Sridhara R, Pazdur R. FDA drug approval summary: erlotinib (Tarceva) tablets. Oncologist. 2005;10(7):461–6.
29. Smith NF, Baker SD, Gonzalez FJ, Harris JW, Figg WD, Sparreboom A. Modulation of erlotinib pharmacokinetics in mice by a novel cytochrome P450 3A4 inhibitor, BAS 100. Br J Cancer. 2008;98(10):1630–2.
30. Eli Lilly and Company. GEMZAR® (gemcitabine hydrochloride) for injection. Available from: http://www.accessdata.fda.gov/drugsatfda_docs/label/2010/020509s064lbl.pdf. Accessed 1996.